

Ergodicity and efficiency of cross-polarization in NMR of static solids

Alexander A. Nevzorov

Department of Chemistry, North Carolina State University, 2620 Yarbrough Drive, Raleigh 27695-8204, NC, USA

ARTICLE INFO

Article history:

Received 15 November 2010

Revised 29 December 2010

Available online 13 January 2011

Keywords:

Cross-polarization

Ergodicity

Spin temperature

Quasiequilibria

Many-spin dynamics

Solid-state NMR

ABSTRACT

Cross-polarization transfer is employed in virtually every solid-state NMR experiment to enhance magnetization of low-gamma spins. Theory and experiment is used to assess the magnitude of the final quasi-stationary magnetization amplitude. The many-body density matrix equation is solved for relatively large (up to $N = 14$) spin systems without the spin-temperature assumption for the final spin states. Simulations show that about 13% of the thermodynamic limit is still retained within the proton bath. To test this theoretical prediction, a combination of a reverse cross-polarization experiment and multiple contacts is employed to show that the thermodynamic limit of magnetization cannot be transferred from high- to low-gamma nuclei in a single contact. Multiple contacts, however, fully transfer the maximum magnetization. A simple diffusion on a cone model shows that slow dynamics can affect the build up profile for the transferred magnetization.

© 2011 Elsevier Inc. All rights reserved.

1. Introduction

Since the pioneering work of Hartmann and Hahn [1] and Lurie and Slichter [2] followed by Waugh and co-workers [3] and Ernst and co-workers [4], cross-polarization has become the most essential part of virtually every solid-state NMR experiment. Here the magnetization enhancement for the low-gamma spins is achieved by bringing the dilute spins in equilibrium with the proton bath when the Hartmann–Hahn condition is fulfilled. Several papers describe theories of cross polarization in great detail [5–9]. According to the widely used spin-temperature hypothesis, under the resonant Hartmann–Hahn condition a thermal equilibrium is attained between the low- and high-gamma spin reservoirs. The spin temperatures of the two species in the doubly tilted rotating frame become equalized, and the conservation of energy argument quickly leads to the conclusion that the magnetization enhancement of the low spins is proportional to the ratio of the gamma factor of the high spin to that of the low spin [3]. For instance, when the ^{15}N spins are brought in contact with the abundant protons, the magnetization enhancement of the former is expected to be around 10. Other papers [10–12], however, point out to the existence of universal bounds to spin dynamics that are purely quantum-mechanical in nature. When thermal relaxation is too slow on the time scale of the relevant NMR experiment, they can lead to the limits of allowable polarization transfer that may differ from those obtained from the intuitive thermodynamic arguments based on conservation of energy or entropy of an isolated spin system obeying unitary evolution [13]. Furthermore, Brüschweiler and Ernst

[14,15] noted the existence of non-ergodic quasi-equilibria in short linear chains of like spins, which means that energy is not the only invariant of motion in dipolar-coupled spin systems. The final or “quasi-equilibrium” observable state in those systems strongly depends on the initial condition and relative arrangement of the interacting spins. Thus, the evolution of the spin system is said to be non-ergodic. This behavior, however, can be made ergodic if thermal motions are introduced, i.e. when the distance between the spins are randomly varied at each step of the integration of the Liouville–von Neumann equation describing the evolution of the density matrix, or when the much more general stochastic Liouville equation [16,17] is employed. The currently available computational power allows one to investigate the above important ideas from first principles by involving direct diagonalization of the relevant Hamiltonians for a relatively large number of spins, >10 . More elaborate projection and space restriction techniques allow one to extend the computationally tractable spin space even further, up to 15 and even more spins [18]. The subject of the present paper is to address the classical problem of cross-polarization transfer from directly solving the many-body density matrix equation, and to compare the results to the predictions arising from the spin-temperature hypothesis. Simple solid-state NMR experiments are performed to complement the results of the simulations. Next, we attempt to evaluate the effect of local motions using a simple model of diffusion on a cone to estimate the efficiency of cross polarization in the presence of dynamics. The latter is especially important for solid-state NMR of membrane proteins where dynamic regions may be present, such as the connecting loops or mobile termini, or slow rotational motion of the protein as a whole.

E-mail address: alex_nevzorov@ncsu.edu

2. Cross-polarization transfer in the absence of dynamics

In the classical cross-polarization (CP) experiment, the Hamiltonian operator in the doubly tilted rotating frame [7] can be written as (setting $\hbar = 1$):

$$H = \omega_S S_z + \omega_I I_z^{total} + \sum_{n=1}^{N-1} a_n S_x I_x^{(n)} + \sum_{i<j}^{N-1} b_{ij} \left[\frac{3}{2} I_x^{(i)} I_x^{(j)} - \frac{1}{2} \mathbf{I}^{(i)} \mathbf{I}^{(j)} \right] \quad (1)$$

Here ω_S and ω_I are the radiofrequency (rf) irradiation amplitudes of the low and high spins, respectively. The interaction constants between the low S -spin and $N - 1$ protons (the I spins) are given by a_n , and b_{ij} describe the interactions amongst the protons themselves. When the amplitudes ω_S and ω_I are much larger than the dipolar coupling constants, one can use the truncated Hamiltonian at the exact Hartmann–Hahn match, $\omega_S = \omega_I$:

$$H_T = \frac{1}{4} \sum_{n=1}^{N-1} a_n (S_+ I_-^{(n)} + S_- I_+^{(n)}) - \frac{1}{2} \sum_{i<j}^{N-1} b_{ij} \left[\frac{3}{2} I_z^{(i)} I_z^{(j)} - \frac{1}{2} \mathbf{I}^{(i)} \mathbf{I}^{(j)} \right] \\ \equiv H_{\pm} - \frac{1}{2} H_{like} \quad (2)$$

Using the formal solution for the density matrix equation, we write for the time evolution of the normalized cross-polarization build-up on the S -spin:

$$G(t) = \frac{\text{Tr}(S_z e^{-iH_T t} \alpha I_z e^{iH_T t})}{\text{Tr}(S_z^2)} = \frac{\alpha}{2^{N-2}} \text{Tr}(S_z e^{-iH_T t} I_z e^{iH_T t}) \\ = \frac{\alpha}{2^{N-2}} \text{Tr}[S_z e^{-iH_T t} (S_z + I_z - S_z) e^{iH_T t}] \\ = \alpha \left[1 - \frac{\text{Tr}(S_z e^{-iH_T t} S_z e^{iH_T t})}{2^{N-2}} \right] \quad (3)$$

Here the factor $\alpha \equiv \gamma_I \hbar B_0 / k_B T$ arises from the initial equilibrium density matrix of the I spins, $\rho(0) = \alpha I_z$, “Tr” stands for the matrix trace, and we have used the fact that the operator $(S_z + I_z)$ commutes with H_T . $T_{1\rho}$ relaxation effects have been neglected for the typical lengths of CP contacts employed in solid-state NMR experiments (several milliseconds). Following Waugh [13], we expand the Hamiltonian in terms of its eigenvectors and eigenvalues:

$$G(t) = \alpha \left[1 - \frac{\text{Tr} \sum_{k,j} S_z e^{-i(\lambda_k - \lambda_j)t} |k\rangle \langle k| S_z |j\rangle \langle j|}{2^{N-2}} \right] \\ = \alpha \left[1 - \frac{\sum_{k,j} S_z e^{-i(\lambda_k - \lambda_j)t} |j\rangle \langle j| S_z |k\rangle \langle k|}{2^{N-2}} \right] \quad (4)$$

A key realization comes from the fact that H_T is an even centrosymmetric matrix, due to the presence of the proton–proton interaction Hamiltonian H_{like} of Eq. (2), or, in its explicit matrix form, $\mathbf{1} \otimes \mathbf{H}_{like}$, where $\mathbf{1}$ is a 2×2 unit matrix. Therefore, its eigenvectors will be either symmetric or skew-symmetric [19]. As a result, the diagonal matrix elements for $j = k$ will vanish for any eigenvector. Indeed, for every symmetric or skew-symmetric vector of the general form $v = x \pm Jx$, where J is a permutation matrix having all ones in its secondary diagonal and zeros elsewhere, we have:

$$v^+ S_z v = (x \pm Jx)^+ S_z (x \pm Jx) = x^+ S_z x + x^+ J S_z J x \pm x^+ J S_z x \pm x^+ S_z J x = 0 \quad (5)$$

since $J S_z J = -S_z$ and $J^2 = 1$. Consequently, when we invoke time averaging to determine the quasi-equilibrium (terminal) value of $G(\infty)$, all the diagonal and oscillatory terms vanish except for the case of degenerate eigenvalues, $\lambda_k = \lambda_{k'}$. Thus, we obtain:

$$\bar{G}(\infty) = \alpha \left(1 - \frac{\sum_k |k\rangle \langle k| S_z |k\rangle \langle k|}{2^{N-2}} \right) \leq \alpha \quad (6)$$

Here the summation is carried over the values of k together with the indices k' that correspond to the same eigenvalue, λ_k . Since every term in the summation is non-negative, the thermodynamic limit for the polarization transfer, α , can only be achieved when all the terms in the sum are identically zero, which is unlikely. Therefore, this quantum mechanical treatment is in an apparent contradiction with the result based on the thermodynamic arguments, although this contradiction is not as striking as the magic echoes [20], for example.

The thermodynamic limit can nevertheless be achieved if multiple contacts with the proton reservoir are invoked. This can be accomplished using a modified version of the original multiple-contact experiment [3] as shown in Fig. 3b. Between the contacts, the low-gamma spin magnetization (i.e. the terms corresponding to the operator S_z) is stored along the z -axis owing to its very long T_1 relaxation (typically tens of seconds or longer as observed for the ^{15}N spins). During a sufficiently long wait time between the contacts, the proton T_1 relaxation destroys multiple quantum coherences, and the equilibrium magnetization of the S -spin after an n 'th contact is given by the following recursion relation (ignoring the T_1 relaxation of the low-gamma spins):

$$G_n(\infty) = \frac{\text{Tr}\{S_z e^{-iH_T t} [\alpha I_z + G_{n-1}(\infty) S_z] e^{iH_T t}\}}{\text{Tr}(S_z^2)} \Bigg|_{t \rightarrow \infty} \\ = \frac{\text{Tr}(S_z e^{-iH_T t} \alpha I_z e^{iH_T t})}{2^{N-2}} \Bigg|_{t \rightarrow \infty} + G_{n-1}(\infty) \\ - G_{n-1}(\infty) \frac{\text{Tr}(S_z e^{-iH_T t} I_z e^{iH_T t})}{\text{Tr}(S_z^2)} \Bigg|_{t \rightarrow \infty} \quad (7)$$

The first term is just $G_1(\infty)$, $G_0(\infty) = 0$, and the above relation can be rewritten as:

$$G_n(\infty) = G_1(\infty) + G_{n-1}(\infty) [1 - G_1(\infty)/\alpha] \quad (8)$$

which can be summed up as a geometric progression to yield:

$$G_n(\infty) = G_1(\infty) \frac{1 - [1 - G_1(\infty)/\alpha]^n}{1 - [1 - G_1(\infty)/\alpha]} \rightarrow \alpha (n \rightarrow \infty) \quad (9)$$

For instance, if $G_1(\infty)/\alpha = 0.9$, after just two multiple contacts 99% of the thermodynamic limit will be transferred.

3. Cross-polarization in the presence of dynamics

When the Hamiltonian is time dependent, the ensemble-averaged solution is obtained using superoperators and the vec -operator. Due to the fact that the Liouville–von Neumann equation has a form of the Lyapunov matrix equation, $AXB^T + CXD^T = Q$, its formal solution can be written as:

$$\langle vec \rho(t) \rangle = \left\langle \exp_0 \left\{ i \int_0^t L(t') dt' \right\} vec \rho(0) \right\rangle \quad (10)$$

The vec operation simply stacks up the column vectors of the density matrix to form a total vector of 4^N elements, and $vec(AXB^T) = (B \otimes A) vec X$, where “ \otimes ” stands for the Kronecker product. The symbol “ \mathcal{O} ” denotes the Dyson time ordering. The Liouvillian “commutator superoperator” $L(t)$ is given by:

$$L(t) = H_T(t) \otimes \mathbf{1}_{2^N} - \mathbf{1}_{2^N} \otimes H_T(t) \quad (11)$$

Here $\mathbf{1}_{2^N}$ is a unit matrix of the size $2^N \times 2^N$. The solution for the magnetization transfer is then given by the scalar product:

$$G(t) = (vec S_z)^T \langle vec \rho(t) \rangle \quad (12)$$

For the motions that have sufficiently short correlation time compared to the variation of $G(t)$, the solution can be truncated using

the generalized cumulant expansion [21,22] up to the second order, which yields:

$$\langle \text{vec } \rho(t) \rangle = \exp_0 \left\{ i \int_0^t dt' \langle L(t') \rangle - \int_0^t dt' \int_0^{t'} dt'' [\langle L(t')L(t'') \rangle - \langle L(t') \rangle \langle L(t'') \rangle] + \dots \right\} \text{vec } \rho(0) \quad (13)$$

For a Markov process, the correlation function depends only on the difference $\tau = t' - t''$, and in the short correlation time limit we obtain:

$$\langle \text{vec } \rho(t) \rangle = \exp_0 \left\{ it \langle L(t) \rangle - \int_0^t d\tau (t - \tau) [\langle L(\tau)L(0) \rangle - \langle L(\tau) \rangle \langle L(0) \rangle] \right\} \text{vec } \rho(0) \\ \approx \exp \left\{ it \langle L(t) \rangle - t \int_0^\infty d\tau [\langle L(\tau)L(0) \rangle - \langle L(\tau) \rangle \langle L(0) \rangle] \right\} \text{vec } \rho(0) \quad (14)$$

The first term in the exponential superoperator is just the Liouvillian, Eq. (11), albeit with time-averaged coupling constants scaled by the local order parameters. If the motions of the spins are assumed to be stochastically independent, the second term contains the squares of superoperators corresponding to the interactions for each pair of spins multiplied by a quantity having the meaning of spectral density. Clearly, considering both many-body spin dynamics and the motions of all spins at the same time is a daunting task [23]. Therefore, for simplicity, let us consider the motion of only one bond between the *S*-spin and its covalently bonded proton, and neglect the motion of the bath protons. Correlations to the distant protons decay quickly as their distance to the nitrogen spin increases. As the next approximation, we describe the restricted motions of the bond by a simple diffusion-on-a-cone model. The interaction constants a_n in Eq. (2) can be written in terms of the second-rank spherical harmonics:

$$a_n = \chi \sqrt{\frac{16\pi}{5}} Y_0^{(2)}(\theta_n, \varphi_n) \quad (15)$$

Here the coupling constant (in rad s^{-1}) is given by: $\chi = (\mu_0/4\pi)(\gamma_I\gamma_S \hbar/r_{IS}^3)$, where γ_I and γ_S are the gyromagnetic ratios of the high and low spin, respectively, and r_{IS} is the interspin distance. Since the motion of only one bond (with the first proton) will be considered, we shall omit the index n in the subsequent equations. To calculate the correlation function we use the following transformation property of the spherical harmonics:

$$Y_0^{(2)}(\theta, \varphi) = \sum_{m=-2}^2 Y_m^{(2)}(\theta_B, \phi_B) D_{m0}^{(2)}(\alpha, \beta, \gamma) \quad (16)$$

Here θ_B is the bond angle with respect to the axis of the cone, φ_B is the random azimuthal angle, and the Euler angles α, β, γ in the Wigner matrix $D^{(2)}(\alpha, \beta, \gamma)$ define the orientation of the cone relative to the laboratory frame. The total correlation function corresponding to the motion of the bond can, therefore, be decomposed as:

$$\langle Y_0^{(2)}(\theta(\tau), \varphi(\tau)) Y_0^{(2)}(\theta(0), \varphi(0)) \rangle \\ = \sum_{m=-2}^2 \langle Y_m^{(2)}(\theta_B, \phi_B(\tau)) Y_{-m}^{(2)}(\theta_B, \phi_B(0)) \rangle d_{m0}^{(2)}(\beta) d_{-m0}^{(2)}(\beta) \quad (17)$$

The individual correlation functions are calculated by standard methods as [24]:

$$\langle Y_m^{(2)}(\theta_B, \phi_B(\tau)) Y_{-m}^{(2)}(\theta_B, \phi_B(0)) \rangle \\ = \int_0^{2\pi} d\phi_B \int_0^{2\pi} d\phi_B^{(0)} Y_m^{(2)}(\theta_B, \phi_B) Y_{-m}^{(2)}(\theta_B, \phi_B^{(0)}) P(\phi_B, \phi_B^{(0)}, \tau) P(\phi_B^{(0)}) \quad (18)$$

Here $p(\phi_B^{(0)}) = 1/2\pi$, is the initial distribution function. The probability density $P(\phi_B, \phi_B^{(0)}, \tau)$ is obtained from the solution of the

isotropic angular diffusion equation in φ having a diffusion coefficient D_{\parallel} :

$$P(\phi_B, \phi_B^{(0)}, \tau) = \frac{1}{2\pi} \sum_{m=-\infty}^{+\infty} e^{im(\phi_B - \phi_B^{(0)})} e^{-D_{\parallel} m^2 \tau} \quad (19)$$

Explicit integration over the angles and using the expressions for the reduced Wigner matrix elements, $d_{mm'}^{(2)}(\beta)$, yields:

$$\langle Y_0^{(2)}(\theta(\tau), \varphi(\tau)) Y_0^{(2)}(\theta(0), \varphi(0)) \rangle \\ = \frac{5}{16\pi} \left[(3 \cos^2 \theta_B - 1)^2 \frac{(3 \cos^2 \beta - 1)^2}{4} + \frac{9}{8} e^{-D_{\parallel} \tau} \sin^2 2\theta_B \sin^2 2\beta \right. \\ \left. + \frac{9}{8} e^{-4D_{\parallel} \tau} \sin^4 \theta_B \sin^4 \beta \right] \quad (20)$$

Time integration of the total correlation function in the second-order cumulant gives rise to the zero-field spectral density:

$$J(0) \equiv \int_0^\infty d\tau [\langle Y_0^{(2)}(\theta(\tau), \varphi(\tau)) Y_0^{(2)}(\theta(0), \varphi(0)) \rangle \\ - \langle Y_0^{(2)}(\theta(\tau), \varphi(\tau)) \rangle \langle Y_0^{(2)}(\theta(0), \varphi(0)) \rangle] \\ = \frac{5}{16\pi} \frac{9}{8D_{\parallel}} \left[\sin^2 2\theta_B \sin^2 2\beta + \frac{1}{4} \sin^4 \theta_B \sin^4 \beta \right] \quad (21)$$

For instance, setting $\beta = \pi/2$ would correspond to the perpendicular orientation of a membrane protein relative to the main magnetic field, such as observed in magnetically aligned bicelles [25]. Here the coupling constants in the time-averaged Liouvillian of Eq. (14) are scaled by the order parameter $(3 \cos^2 \beta - 1)/2 = -0.5$. Due to the symmetric nature of Eq. (21) the angle β can also be treated as the amplitude of the local motions confined to the surface of the cone when its average orientation is described by the static bond angle, θ_B . More complicated models describing restricted motions of the spins can also be considered [26,27]. The solution for the ensemble-averaged density matrix can therefore be written in an explicit matrix-vector form:

$$\langle \text{vec } \rho(t) \rangle = \exp\{t[i\langle L(t) \rangle - \chi^2 J(0)C^2]\} \text{vec } \rho(0) \quad (22)$$

where the superoperator matrix C is given by:

$$C = \frac{(S_+ I_-^{(1)} + S_- I_+^{(1)})}{4} \otimes \mathbf{1}_{2^N} - \mathbf{1}_{2^N} \otimes \frac{(S_+ I_-^{(1)} + S_- I_+^{(1)})}{4} \quad (23)$$

It should be noted that Eq. (22) describes evolution under the time-averaged many-body Hamiltonian as well as relaxation due to motions, and the time evolution is no longer unitary.

4. Results

4.1. Simulations

Simulations were performed using synthetic coordinates of an ideal polyaniline α -helix tilted at 30° with respect to the main magnetic field. Fig. 1 shows simulations including single nitrogen coupled to the various numbers of protons as indicated. The magnetization at the nitrogen spin has been calculated from Eq. (3) in units of α using a MATLAB script. For Fig. 1d ($N = 14$ spins), direct diagonalization was not possible, and the “expv” routine was used instead [28]. As can be seen, the quasiequilibrium fluctuation amplitudes decrease with the increasing number of protons. Moreover, regardless of the number of protons considered, the quasistationary magnetization amplitude at the nitrogen spins never reaches the thermodynamic value, α . The quasistationary (time-averaged) magnetization amplitudes have been calculated directly from Eq. (6) and can be compared to the values obtained from the plots. For $N = 8$ spins, Eq. (6) yields: 0.8097; and thereafter shows a

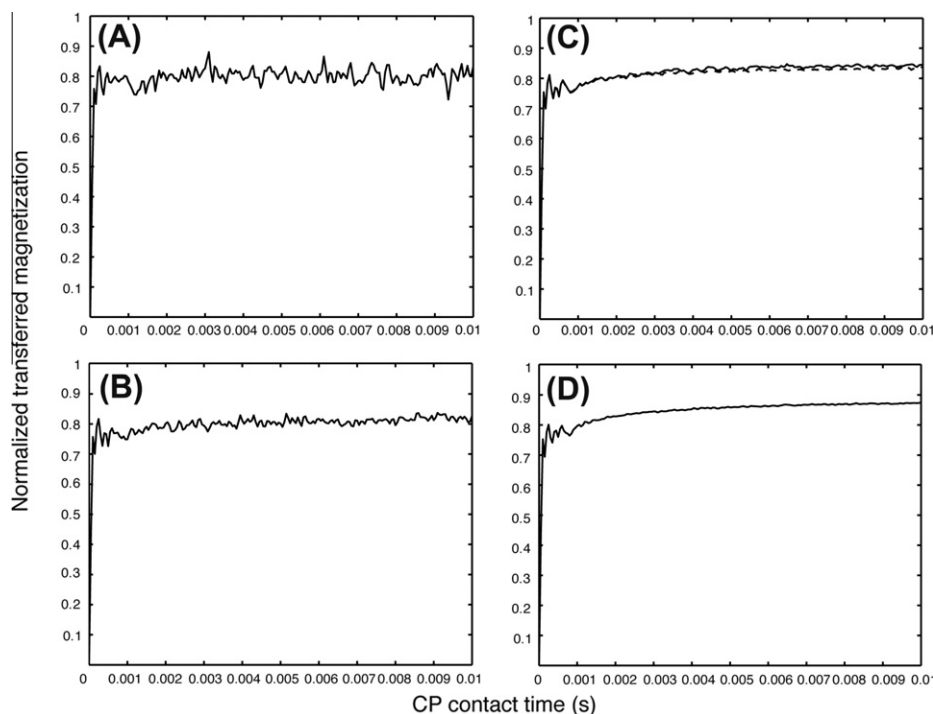


Fig. 1. Cross-polarization build-up as a function of the number of spins in the simulation. (A) 8 Spins. (B) 10 Spins. (C) 12 Spins. (D) 14 Spins. The amplitude of quasi-equilibrium fluctuations decreases as the number of spins in the system increases; whereas the quasistationary magnetization never reaches the thermodynamic limit (normalized to 1). In part (C), dashed line shows simulation with the full Hamiltonian, Eq. (1), with $\omega_I = \omega_S = 100$ kHz.

slight tendency towards higher values as the number of spins in the simulation increases: 0.8179 ($N = 10$); 0.8494 ($N = 12$); and 0.8648 ($N = 13$). Interestingly, for an adiabatic transfer, Sørensen reports [11] convergence to the factor 0.8 relative to the value obtained from the conservation of entropy argument. In addition, Fig. 2c demonstrates close agreement between the simulations using the full Hamiltonian, Eq. (1) (dashed line) and its truncated variant, Eq. (2) (solid line). Fig. 2 shows simulations in the presence of local dynamics as described by Eqs. (12) and (22). Calculations were done using the “expv” routine [28]. Fig. 2a shows a two-spin ($N = 2$) simulation using Eq. (22) for $D_{||} = 10^6 \text{ s}^{-1}$, $\beta = 90^\circ$, which corresponds to the timescale of uniaxial diffusion of a membrane protein in magnetically aligned bicelles [25]. In this case relaxation drives the magnetization to the final value of 0.5. When a bath of 8 protons is added ($N = 10$), the effect of local dynamics becomes less pronounced, cf. Fig. 2b. Here the final magnetization slightly increases as compared to the solution obtained from the static Hamiltonian with time-averaged coupling constants (dashed line). The

increase in the transferred magnetization becomes even more dramatic in Fig. 2c, where $D_{||} = 10^5 \text{ s}^{-1}$ which is likely at the limit of the short correlation time approximation, Eq. (14). However, when $D_{||}$ is increased to 10^9 s^{-1} and $\beta = 10^\circ$ in Fig. 2c, which could be used to model internal fluctuations of the N–H bonds, for example, the effect of local dynamics on the CP transfer becomes negligible (results not shown). In this fast motional limit, the dipolar couplings are simply scaled by the motional order parameters, which do not affect the final amount of the transferred magnetization, only the transfer rate.

4.2. Experimental

In the present work, a small (0.7 mg) ^{15}N -labeled single crystal of *n*-acetyl Leucine was used, which exhibits four sharp resolved resonances corresponding to four distinct orientations of the N–H bonds. Direct experimental determination of the efficiency of cross polarization is in general difficult. For instance, ^{15}N spins in single

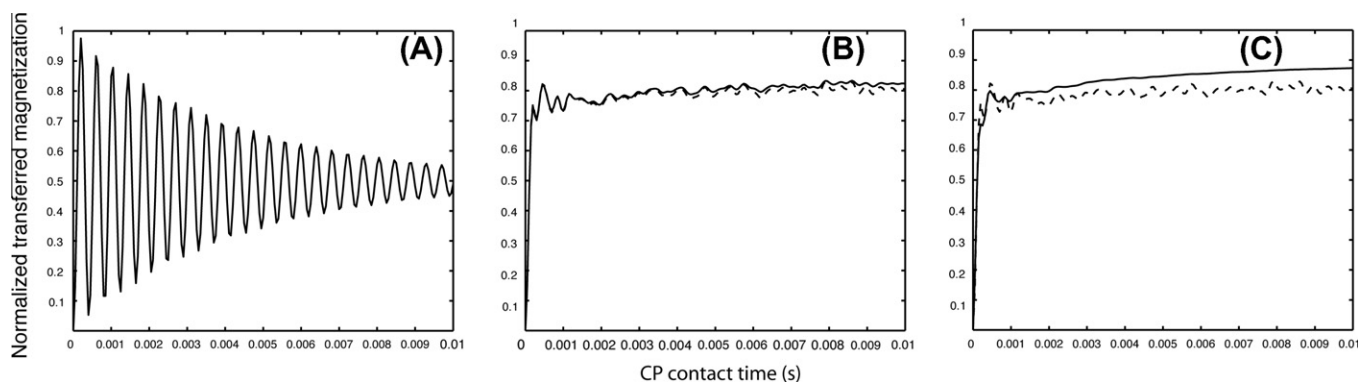


Fig. 2. Effect of slow dynamics on CP build-up curves. (A) Two-spin case, $D_{||} = 10^6 \text{ s}^{-1}$, $\beta = 90^\circ$; (B) 10-spin case, $D_{||} = 10^6 \text{ s}^{-1}$, $\beta = 90^\circ$; (C) 10-spin case, $D_{||} = 10^5 \text{ s}^{-1}$, $\beta = 90^\circ$. In parts (B) and (C) the dashed lines shows the solution obtained with time-averaged coupling constants for comparison (cf. the text).

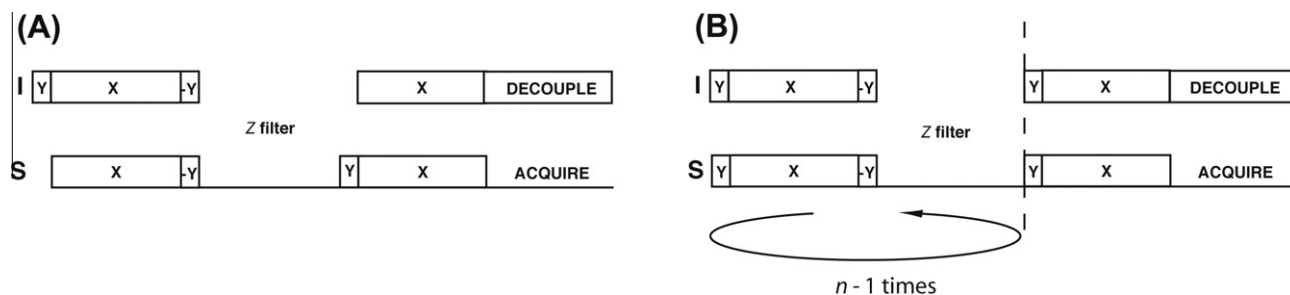


Fig. 3. Pulse sequences used in the NMR experiments. (A) Inverse CP; (B) Multiple-contact CP. During the z-filter (typically applied for several seconds) the proton spins fully relax to thermal equilibrium; whereas the nitrogen magnetization is stored along the z-axis due to its much longer T_1 relaxation time.

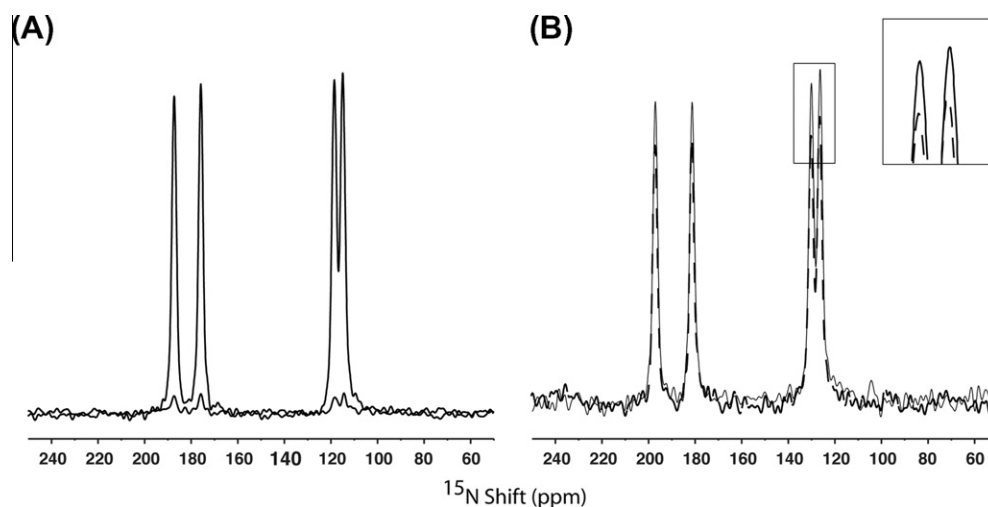


Fig. 4. (A) Inverse CP experiment for an NAL crystal at arbitrary orientation showing residual magnetization on the nitrogen spins obtained using the pulse sequence of Fig. 3a as compared to a single-contact CP spectrum (2 k scans; 3 s z-filter; 5 ms contact times; $\omega_I = \omega_S = 56$ kHz). (B) Comparison of multiple-contact experiment (Fig. 3b) with single-contact CP for an NAL crystal at arbitrary orientation (128 scans; 4 s z-filter; $\omega_I = \omega_S = 56$ kHz; 1 ms contact time for six multiple contacts and 5 ms for the single CP). Multiple contacts allow one to transfer additional magnetization to the nitrogen spins.

crystalline species can hardly be detected owing to their low gamma ratio, on the one hand, and a very long T_1 relaxation time (on the order of tens of seconds), on the other. Therefore, here we use an indirect method depicted in Fig. 3a. After the initial CP contact, both the nitrogen spins and the protons are brought along the z-axis, and a wait time of several seconds is applied to thermally equilibrate the proton spins. Then only the nitrogen spins are flipped back in the direction of the x-axis, followed by their simultaneous irradiation together with the proton spins under the Hartmann–Hahn condition. If full thermal equilibration indeed occurs in such a “reverse CP” experiment, there should be no detectable magnetization left on the low spins. Contrary to this expectation, however, an appreciable magnetization still remains as can be seen from Fig. 4a. To check whether this might be a consequence of a Hartmann–Hahn mismatch, additional measurements have been performed by varying the rf amplitude of the low spins near the experimentally determined Hartmann–Hahn condition, which exhibited equal or greater residual magnetization on all four resonances (results not shown). Next, multiple contacts (cf. Fig. 3b) between the low- and high-gamma reservoirs were employed to overcome the quantum mechanical limit of a single cross-polarization contact. Here, the magnetization is transferred back and forth between the spins until the thermodynamic limit is achieved. As can be seen from Fig. 4b (inset), additional magnetization can indeed be transferred. The number of contacts has

been varied from 2 to 6, which yielded similar intensities of the spectra. From integrating the spectra in Fig. 4a, the residual magnetization remaining at the nitrogen spins after the inverse CP experiment is calculated to be at around 8% relative to a single-CP transfer. On the other hand, the integral ratio of the two spectra in Fig. 4b is about 1.2, from which the amount of the residual magnetization after the inverse CP contact is calculated to be at 17%. The sum factor calculated from Eq. (6) is around 13% for a system of 13 spins, which places it between the two experimental values (it should be noted, however, that a slight trend in the increase of the transferred amplitude with the number of spins is observed in the simulations).

5. Conclusions

In the classical cross-polarization scheme of static crystalline solids, thermal equilibrium in the doubly tilted rotating frame cannot be established within the timescale of a single transfer (typically several milliseconds). This would imply that the spin system does not have sufficient time to exchange its energy quanta with the lattice having an astronomical number of degrees of freedom. As a result, within the timescale of the cross-polarization experiment, a Boltzmann distribution is not established in such an isolated spin system. It has been shown both quantum-

mechanically and experimentally that at least 8% of the residual magnetization remains on the low spins after a single cross-polarization contact with the unpolarized proton bath. By inverse argument, we conclude that the full thermodynamic limit cannot be transferred to the low spins from the high spins in a single CP experiment. However, the thermodynamic limit can be achieved through multiple contacts via thermal relaxation of the multiple quantum coherences formed after each CP step. Generalized cumulant expansion together with the vectorization of the density matrix represents a convenient and compact way of treating random time-dependent Hamiltonians. It has been found that local dynamics modeled as a simple diffusion on a cone can affect the final equilibrium magnetization and the amplitude of transient oscillations when the motions are sufficiently slow. This, in turn, may allow one to extract dynamic information for macroscopically oriented samples such as membrane proteins from a detailed analysis of their CP build-up curves.

Acknowledgments

The author would like to thank Profs. Rafael Brüschweiler (FSU and NHFML) and Alex I. Smirnov (NCSSU) for the critical reading of the manuscript and valuable comments. Supported by grants MCB 0843520 from NSF and North Carolina Biotechnology Center.

References

- [1] S.R. Hartmann, E.L. Hahn, Nuclear double resonance in the rotating frame, *Phys. Rev.* 128 (1962) 2042–2053.
- [2] F.M. Lurie, C.P. Slichter, Spin temperature in nuclear double resonance, *Phys. Rev. Lett.* 10 (1963) 403.
- [3] A. Pines, M.G. Gibby, J.S. Waugh, Proton-enhanced NMR of dilute spins in solids, *J. Chem. Phys.* 59 (1973) 569–590.
- [4] L. Müller, A. Kumar, T. Baumann, R.R. Ernst, Transient oscillations in NMR cross-polarization experiments, *Phys. Rev. Lett.* 32 (1974) 1402–1406.
- [5] D.E. Demco, J. Tegenfeldt, J.S. Waugh, Dynamics of cross relaxation in nuclear magnetic double-resonance, *Phys. Rev. B* 11 (1975) 4133–4151.
- [6] M.H. Levitt, D. Suter, R.R. Ernst, Spin dynamics and thermodynamics in solid-state NMR cross polarization, *J. Chem. Phys.* 84 (1986) 4243–4255.
- [7] M. Levitt, Heteronuclear cross polarization in liquid-state nuclear magnetic resonance: mismatch compensation and relaxation behavior, *J. Chem. Phys.* 94 (1991) 30–38.
- [8] D. Marks, S. Vega, A theory for cross-polarization NMR of nonspinning and spinning samples, *J. Magn. Reson. Ser. A* 118 (1996) 157–172.
- [9] P. Hodgkinson, A. Pines, Cross-polarization efficiency in INS systems using adiabatic RF sweeps, *J. Chem. Phys.* 107 (1997) 8742–8751.
- [10] O.W. Sorensen, Polarization transfer experiments in high-resolution NMR-spectroscopy, *Prog. Nucl. Magn. Reson. Spectrosc.* 21 (1989) 503–569.
- [11] O.W. Sorensen, A universal bound on spin dynamics, *J. Magn. Reson.* 86 (1990) 435–440.
- [12] N.C. Nielsen, O.W. Sorensen, Accessible states in Liouville space – a 2-dimensional extension of the universal bound on spin dynamics applied to polarization transfer in I(N)S(M) spin-1/2 systems, *J. Magn. Reson.* 99 (1992) 449–465.
- [13] J.S. Waugh, Equilibrium and ergodicity in small spin systems, *Mol. Phys.* 95 (1998) 731–735.
- [14] R. Brüschweiler, R.R. Ernst, Non-ergodic quasi-equilibria in short linear spin 1/2 chains, *Chem. Phys. Lett.* 264 (1997) 393–397.
- [15] R. Brüschweiler, Nuclear spin relaxation and non-ergodic quasi-equilibria, *Chem. Phys. Lett.* 270 (1997) 217–221.
- [16] R. Kubo, Stochastic theories of randomly modulated systems, *J. Phys. Soc. Jpn.* 26 (Suppl.) (1969) 1–5.
- [17] J.H. Freed, in L.T. Muus, P.W. Atkins (Eds.), *Electron Spin Relaxation in Liquids*, Plenum Press, New York, 1972, pp. 387–410.
- [18] H.J. Hogben, P.J. Hore, I. Kuprov, Strategies for state space restriction in densely coupled spin systems with applications to spin chemistry, *J. Chem. Phys.* 132 (2010) 174101–174110.
- [19] J.R. Weaver, Centrosymmetric (cross-symmetric) matrices, their basic properties, eigenvalues, and eigenvectors, *Am. Math. Mon.* 92 (1985) 711–717.
- [20] W.-K. Rhim, A. Pines, J.S. Waugh, Time-reversal experiments in dipolar-coupled spin systems, *Phys. Rev. B* 3 (1971) 684–696.
- [21] R. Kubo, Generalized cumulant expansion method, *J. Phys. Soc. Jpn.* 17 (1962) 1100–1120.
- [22] J.H. Freed, Generalized cumulant expansions and spin-relaxation theory, *J. Chem. Phys.* 49 (1968) 376–391.
- [23] A.A. Nevzorov, J.H. Freed, Dipolar relaxation in a many-body system of spins of 1/2, *J. Chem. Phys.* 112 (2000) 1425–1443.
- [24] A. Abragam, *The Principles of Nuclear Magnetism*, Oxford University Press, London, 1961.
- [25] A.A. De Angelis, A.A. Nevzorov, S.H. Park, S.C. Howell, A.A. Mrse, S.J. Opella, High-resolution NMR spectroscopy of membrane proteins in “unflipped” bicelles, *J. Am. Chem. Soc.* 126 (2004) 15340–15341.
- [26] A.G. Palmer, J. Williams, A. McDermott, Nuclear magnetic resonance studies of biopolymer dynamics, *J. Phys. Chem.* 100 (1996) 13293–13310.
- [27] E. Meirovitch, Y.E. Shapiro, A. Polimeno, J.H. Freed, Structural dynamics of biomacromolecules by NMR: the slowly relaxing local structure approach, *Prog. Nucl. Magn. Reson. Spectrosc.* 56 (2010) 360–405.
- [28] R.B. Sidje, Expokit: a software package for computing matrix exponentials, *ACM Trans. Math. Softw.* 24 (1998) 130–156.